Subtype-Specific Mechanisms for Functional Interaction between α6β4* Nicotinic Acetylcholine Receptors and P2X Receptors

Walrati Limapichat, Dennis A. Dougherty, Henry A. Lester

Molecular Pharmacology 2014

SUPPLEMENTAL INFORMATION

Supplemental Table 1. ACh and ATP EC_{50} values from oocytes expressing combinations of α6β4* nAChR and P2X receptors.

Receptor(s)	Dose-response	Additional Agonist	EC_{50}	Hill Constant	*n*
			μM		
α6(L9'S)β4	ACh		3.3 ± 0.11	1.4 ± 0.05	8
α6β4β3(V13'S)	ACh		1.3 ± 0.06	0.84 ± 0.03	10
P2X2	ATP		24 ± 1.2	1.5 ± 0.10	18
α6(L9'S)β4 + P2X2	ACh		4.3 ± 0.10	1.3 ± 0.03	11
	ACh	32 μM ATP	4.5 ± 0.26	1.4 ± 0.09	14
	ACh	100 μM ATP	6.0 ± 0.82	1.5 ± 0.23	14
	ATP		22 ± 1.1	1.6 ± 0.11	11
	ATP	100 μM ACh	33 ± 3.6	1.3 ± 0.15	11
α6β4β3(V13'S) + P2X2	ACh		1.6 ± 0.09	0.84 ± 0.03	12
	ACh	32 μM ATP	2.4 ± 1.1	0.75 ± 0.18	19
	ACh	100 μM ATP	1.6 ± 0.45	0.67 ± 0.09	8
	ATP		23 ± 1.7	1.6 ± 0.15	11
	ATP	100 μM ACh	24 ± 3.1	1.8 ± 0.35	12
P2X3(K65A)	ATP		13.6 ± 1.3	1.4 ± 0.16	12
α6(L9'S)β4 + P2X3(K65A)	ACh		3.3 ± 0.13	1.3 ± 0.06	8
	ATP		37.8 ± 6.1	0.94 ± 0.11	14
	ATP	100 μM ACh	32.8 ± 5.0	1.0 ± 0.12	11
α6β4β3(V13'S) + P2X3(K65A)	ACh		1.1 ± 0.10	0.84 ± 0.05	7
	ATP		7.6 ± 0.33	1.6 ± 0.09	11
	ATP	100 μM ACh	11.5 ± 1.6	1.3 ± 0.21	12
P2X2(T18A)	ATP		24.1 ± 4.8	1.0 ± 0.15	11
α6(L9'S)β4 + P2X2(T18A)	ATP		22.9 ± 2.7	1.1 ± 0.12	11
P2X3TR	ATP		9.73 ± 0.29	1.5 ± 0.06	6
α6(L9'S)β4 + P2X3TR	ATP		20.1 ± 5.3	0.97 ± 0.20	7
	ATP	100 μM ACh	39.0 ± 6.5	1.0 ± 0.13	8

LEGENDS TO SUPPLEMENTAL FIGURES

Supplemental Figure 1. nAChR alone is not activated or modulated by ATP, and P2X receptor alone is not activated or modulated by ACh.

(a) Mean normalized ACh (100 μM), ATP (1 mM), and ACh+ATP currents ± s.e.m. from oocytes injected with P2X2, α6β4, or α6β4β3 (n = 6, 8, and 14, respectively). (b) Mean normalized ACh (100 μM), ATP (100 μM), and ATP* currents from oocytes injected with P2X3 (n =10).

Supplemental Figure 2.

Mean normalized agonist-induced currents ± s.e.m. are shown for P2X2–α6β4 oocytes (n = 12) upon receptor activation by ACh (100 μM), ATP (1 mM), ACh+ATP, ATP (1 mM), and then ACh (100 μM), respectively. The arrow indicates sequential agonist application. All measured current signals were normalized to the current evoked by ACh+ATP of the same cell and then averaged. The data highlight that $1^{st}\ I_{ATP} > 2^{nd}\ I_{ATP}$ while $1^{st}\ I_{ACh} \approx 2^{nd}\ I_{ACh}$.

Supplemental Figure 3. A P2X2 desensitized state may play a role in P2X2–α6β4 cross inhibition.

Representative current traces from oocyte expressing P2X2 only (*left*) and oocyte co-expressing α6β4 and P2X2 (*right*) upon application of 1 mM ATP. P2X2 oocyte shows minimal desensitization whereas P2X2–α6β4 oocyte showed ~20% desensitization.

Supplemental Figure 4. Validation of the "prolonged plus brief pulse" protocol, showing functional interaction between P2X2(T18A) and α6β4 receptors.

(a) Mean, normalized agonist-induced current ± s.e.m. from P2X2(T18A)–α6β4 oocytes (n = 10) upon application of ACh (100 μM), ATP (1 mM), and ATP with ACh pre-application (ATP*). Cross inhibition was observed between P2X2(T18A) and α6β4 at 1mM ATP. All current signals were normalized to the ATP current of the same cell and then averaged. Δ* is the difference between I_{ATP} and I_{ATP*}. ***, $p < 0.0005$. The waveforms resembled those of Figure 4a, inset.

(b) ATP dose-response relations for P2X2(T18A) oocytes (EC_{50} 24.1 ± 4.8 μM, Hill constant 1.0 ± 0.15, n = 11), and P2X2(T18A)–α6β4 oocytes (EC_{50} 22.9 ± 2.7 μM, Hill constant 1.1 ± 0.12, n = 11). The curve fit for wild-type P2X2 oocytes is shown in grey (EC_{50} 23.9 ± 1.5 μM, Hill constant 1.5 ± 0.10, n = 18) as a reference, omitting the data points for clarity. The P2X2(T18A) receptor produced an ATP dose-response relation that is similar to the wild-type P2X2 receptor, despite very different desensitizing kinetics. See Supplemental Table 1.

Supplemental Figure 5. Co-injecting P2X2 and P2X3 into Xenopus oocytes produced heteromeric P2X2/3 receptor expression, and P2X2/3 current could be studied using αβmeATP as an agonist.

(a) Representative agonist-induced currents from an oocyte expressing P2X2 alone when ATP or αβmeATP was applied. αβmeATP at 100 μM did not activate P2X2.

(b) Representative agonist-induced current from an oocyte expressing P2X3 alone, showing fast opening and closing kinetics with both ATP and αβmeATP activation.

(c) Representative agonist-induced currents from oocytes injected with P2X2 and P2X3 mRNA at three different ratios. Heteromeric P2X2/3 receptor was activated by αβmeATP and showed different kinetics from homomeric P2X3 channel. At 1:325 and 1:50 P2X2:P2X3 injection ratios, a mixed waveform from P2X3 and P2X2/3 receptors was observed. At 1:10 ratio, the waveform from P2X2/3 predominates. Therefore, the 1:10 P2X2:P2X3 was the mRNA ratio being used throughout this work.

(d) Mean normalized ACh, αβmeATP, and ACh+αβmeATP currents from oocytes injected with 1:10 P2X2:P2X3 (n = 7). P2X2/3 receptor was not activated or modulated by ACh.

Supplemental Figure 6. The role of the nAChR β3 subunit in cross inhibition

α6β4-containing nAChR and (a) P2X2 or P2X2TR receptors, (b) P2X3 or P2X2(T18A) receptors, and (c) P2X2/3 receptors.

Supplemental Figure 7. Mec blocks α6β4 and α6β4β3 in a voltage-dependent fashion.

(a) Mec dose-response relations recorded from oocytes expressing α6β4 or α6β4β3 at −60 mV as the receptor was activated by 100 μM ACh.

(b–c) Representative current traces from voltage jump experiments on an oocyte expressing α6β4 (b) or α6β4β3 (c). Cells were clamped at −60 mV. Current was recorded in the present of 100 μM

ACh +/− Mec at specified concentration. The voltage was stepped in −20 mV increment from +70 mV to −110 mV. Fraction of Mec block was calculated for each cell and then normalized.

Supplemental Figure 8. Results from control experiments for data presented in Figure 7b and 7d.

Mean normalized currents ± s.e.m. are shown for agonist-induced currents measured from P2X2–α6β4 oocytes ($n = 7$) or P2X2–α6β4β3 oocytes ($n = 8$) in response to ACh (100 μM), ATP (1 mM), and 2 repeating doses of ACh+ATP mixture in the order indicated by the arrows. The first and second ACh + ATP applications produced comparable current responses.

Supplemental Figure 1

a.

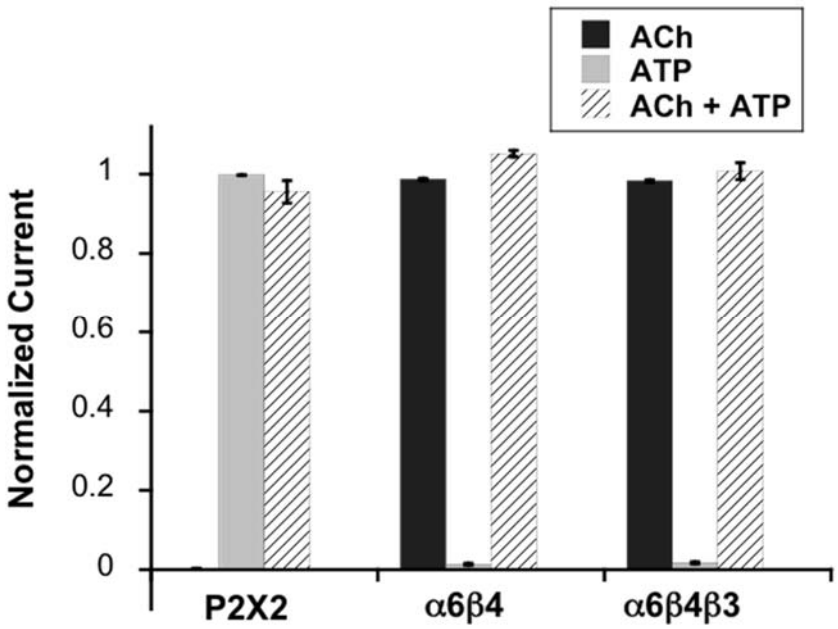

b.

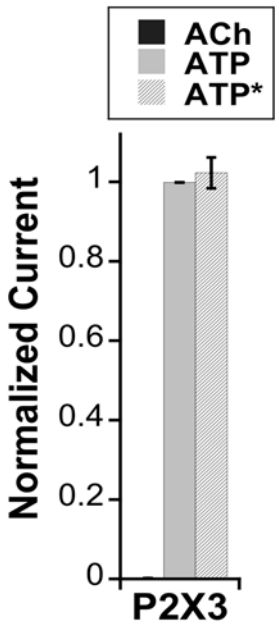

Supplemental Figure 2

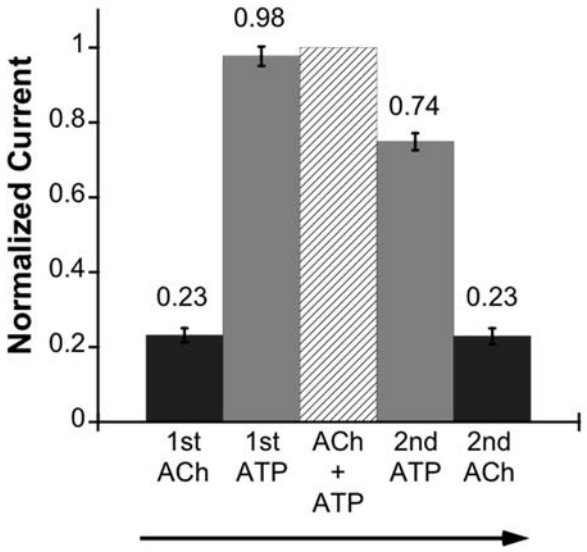

Supplemental Figure 3

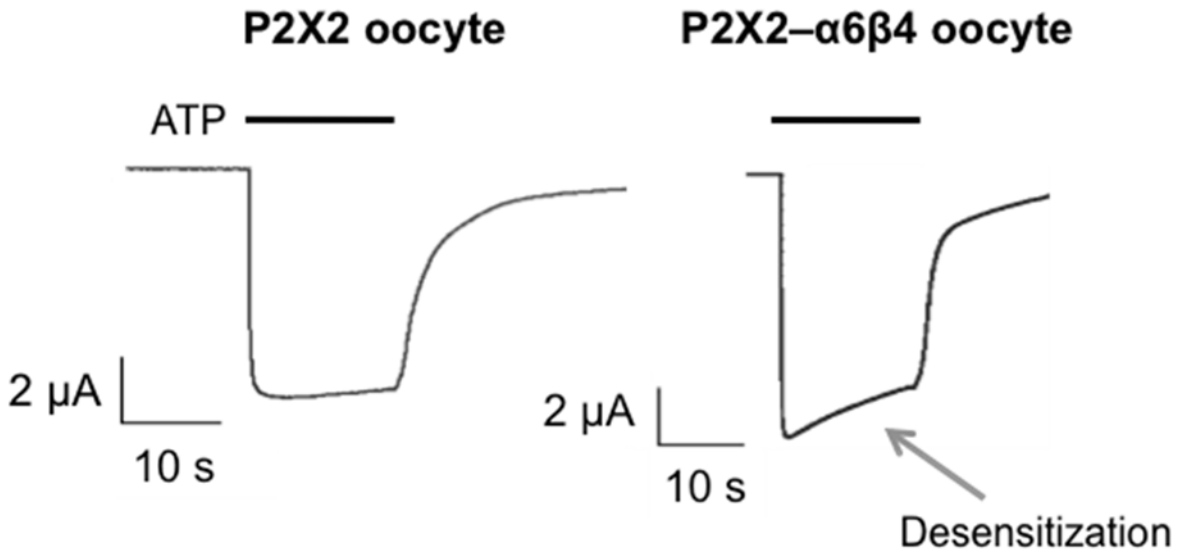

Supplemental Figure 4

a.

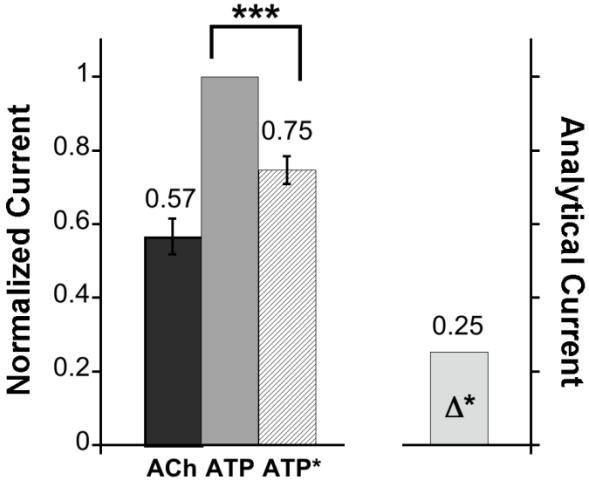

b.

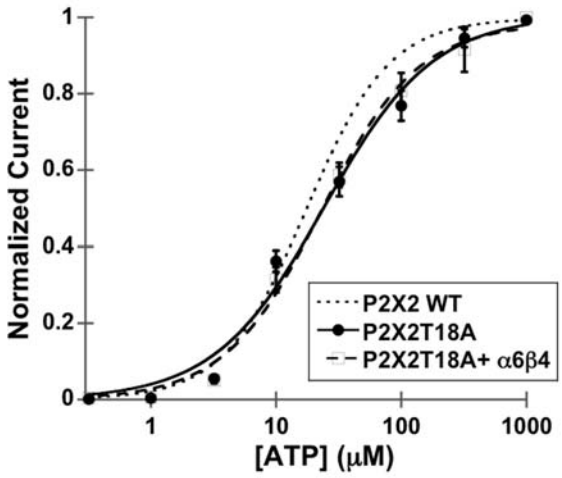

Supplemental Figure 5

a. b.

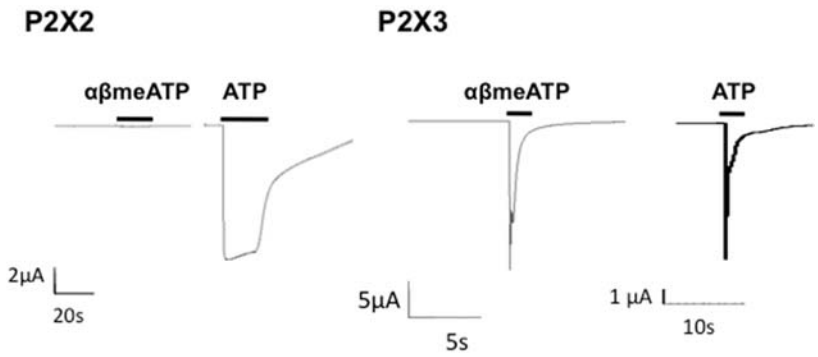

c.

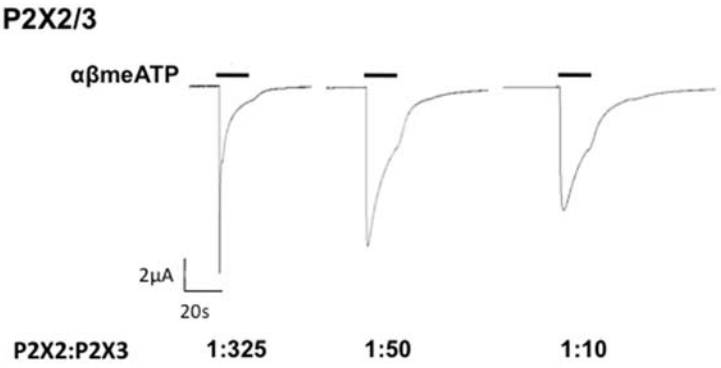

d.

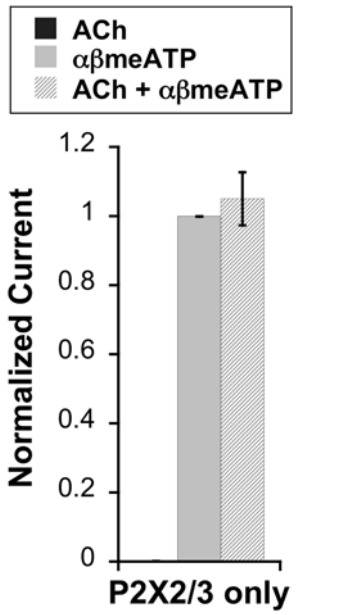

Supplemental Figure 6

a.

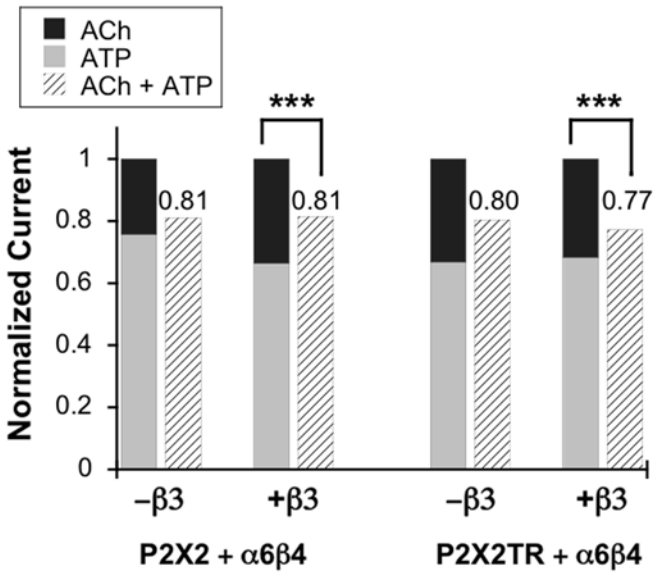

b.

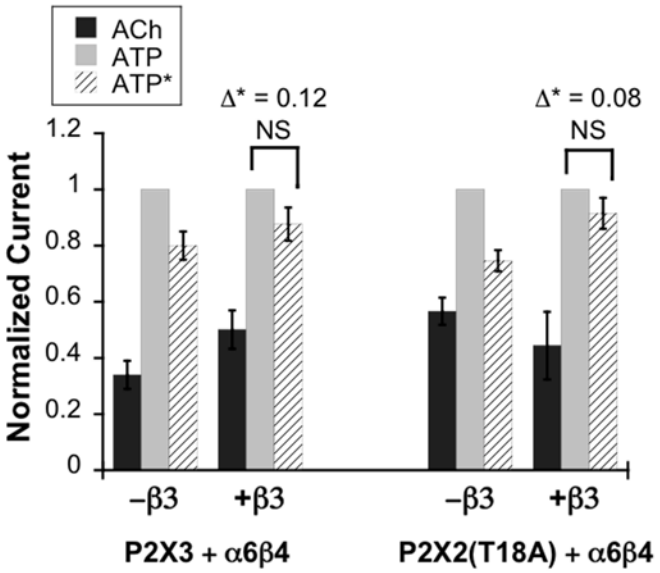

c.

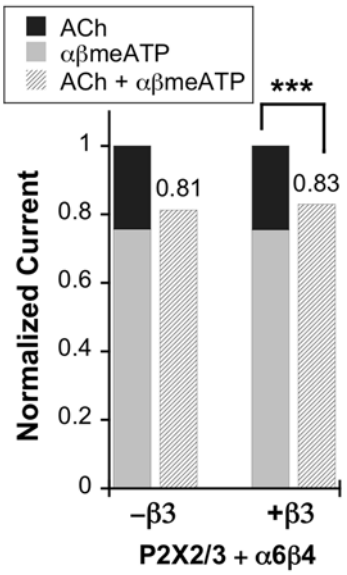

Supplemental Figure 7

a.

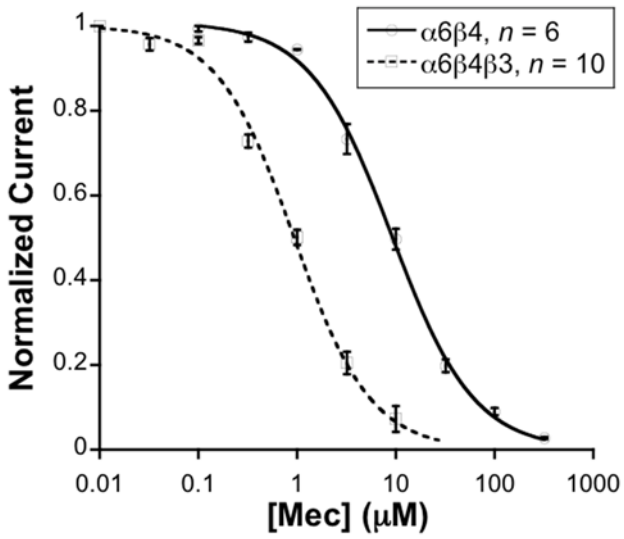

b. α6β4

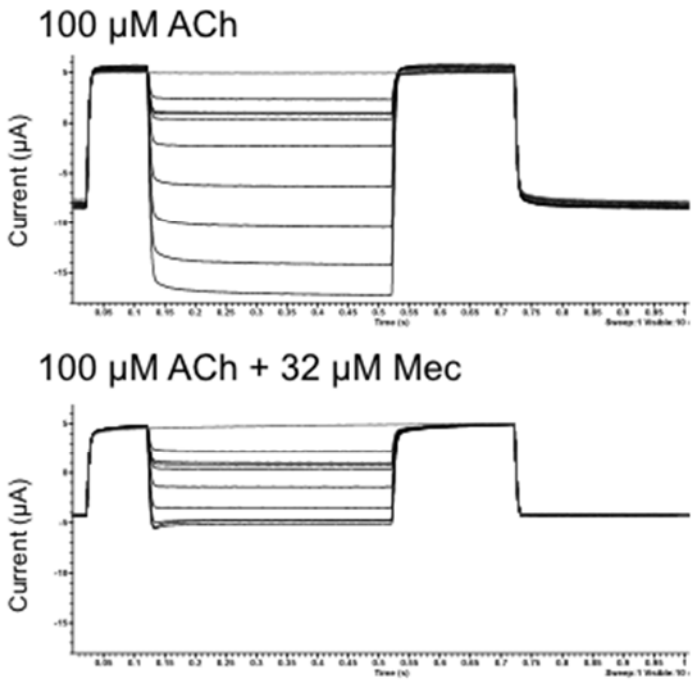

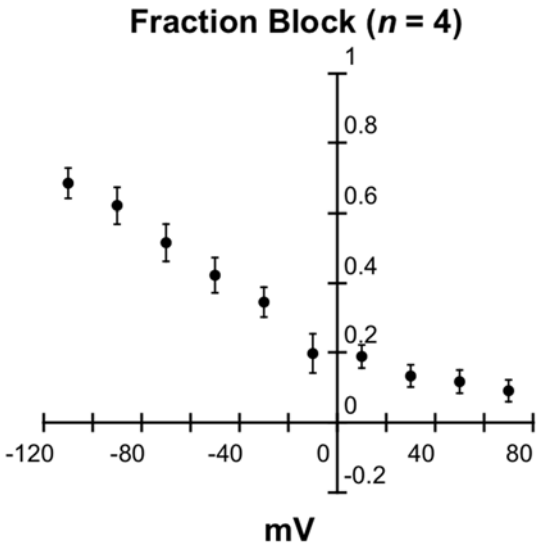

7c. α6β4β3

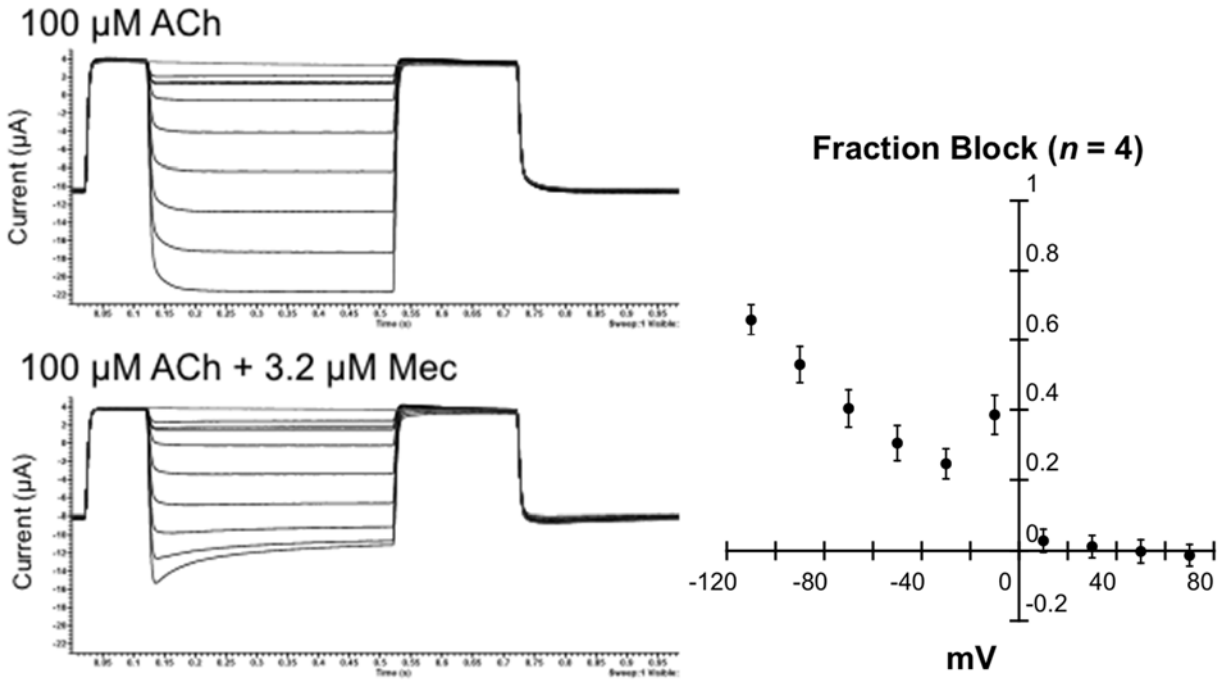
100 µM ACh
Current (µA)
100 µM ACh + 3.2 µM Mec
Current (µA)
Fraction Block (n = 4)
1
0.8
0.6
0.4
0.2
0
-0.2
-120
-80
-40
0
40
80
mV

Supplemental Figure 8